

Measurements of the electron-photon double decay in ^{85}Rb at 30° *

Z. Krečak, K. Ilakovac, and M. Jurčević

Institute "Rudjer Bošković," Zagreb, Yugoslavia

(Received 20 November 1974)

Measurements of the electron-photon double decay of the 514-keV state in ^{85}Rb have been performed at a relative angle of emission of 30° using a fast-slow double coincidence system with a three-dimensional analyzer. The energy spectra of photons and double-decay differential coefficients for $K\gamma$ decay and $(L + M + N)\gamma$ decay have been derived from the counting rates. The results are in agreement with the theory of the internal Compton effect of Spruch and Goertzel.

RADIOACTIVITY $^{85}\text{Rb}^m$; measured $e\gamma$ double decay at 30° ; deduced photon energy distribution in the range 20 to 132 keV for $K\gamma$ decay and 28 to 132 keV for $(L + M + N)\gamma$ decay.

INTRODUCTION

Detailed measurements of the energy and angular distributions in $e\gamma$ double decay have been performed for the 662-keV isomeric transition in ^{137}Ba ¹ and for the 392-keV isomeric transition in ^{113}In .^{2,3} Comparison of the experimental results for these almost pure $M4$ transitions with the theories of $e\gamma$ decay^{4,5} showed that the dominant contribution to the observed results is due to the internal Compton effect ($e\gamma$ decay involving electronic intermediate states). The contribution of nuclear $e\gamma$ decay⁶ was estimated to be smaller than the uncertainty of the measurements. It is of interest to check whether the agreement is also good for transitions of different multipolarity or type and to find conditions under which "nuclear" $e\gamma$ decay could be measured.

The decay scheme of ^{85}Sr , as given in a recent review,⁷ is shown in Fig. 1. The 65-day ground state of ^{85}Sr decays by electron capture to the second excited state at 514 keV in ^{85}Rb , with a very weak branch to the third excited state at 868.5 keV. The experimental value of the K conversion coefficient for the 514-keV transition, $\alpha_K = 0.007 \pm 0.001$, is in agreement with both the $M2$ assignment ($\alpha_K = 0.0064$) and the $E3$ assignment ($\alpha_K = 0.0081$). However, from the half-life of the 514-keV state, $T = 0.958 \pm 0.012 \mu\text{s}$ (a recent precision measurement⁸ gave a value of $1.015 \pm 0.001 \mu\text{s}$), the $E3$ admixture was estimated to be very small (the enhancement factor for a pure $E3$ transition would be about 300). Hence, this transition is considered to be an almost pure $M2$ transition.

The transition probabilities for $e\gamma$ decay were expected to be very small because of the very small conversion coefficient. However, the 514-keV transition in ^{85}Rb is very suitable for studying double-decay processes because of the absence of cascaded emissions.⁹ An attempt was made to

detect $\gamma\gamma$ decay, and an upper limit of $T_{\gamma\gamma}/T_\gamma < 1.2 \times 10^{-5}$ was obtained.¹⁰

MEASUREMENTS

A fast-slow coincidence system was used for measurements of double coincidences of pulses from an electron and a photon detector. The amplitudes of pulses from the detectors and their time difference were recorded on punched paper tape by means of a three-dimensional analyzer. The system was almost identical to the system used in double-coincidence measurements described in Ref. 2.

A 0.5 N HCl solution of SrCl_2 with ^{85}Sr of a radioactive purity of 99% and an initial specific activity of 4.35 mCi/mg (supplied by NEN Corporation, Boston, Massachusetts) was used to prepare the sources. Films of Zapon about $70 \mu\text{g}/\text{cm}^2$ thick were used as backings. To reduce effects of electrostatic charges, strips of aluminum 5 mm wide and $15 \mu\text{g}/\text{cm}^2$ thick were evaporated onto the Zapon films. In each preparation, a droplet of the solution was placed upon the backing. After drying, the spots were about 5 mm in diameter and the average thickness of SrCl_2 was about $10 \mu\text{g}/\text{cm}^2$.

Two arrangements were used in the measurements. They differed in the strengths of the sources, in the electron detectors, and in the distances of the photon detector from the source. In both arrangements the source and the electron detector were mounted inside a vacuum chamber on a plate which was cooled by a dipstick immersed in liquid nitrogen. A coaxial Ge(Li) detector with a sensitive volume of 34 cm^3 (made in the "Boris Kidrič" Institute, Belgrade) was used to detect photons. It was placed outside the chamber, in front of a window in the wall of the vacuum chamber, made of an aluminium foil 0.2 mm thick.

In the first arrangement a silicon surface-bar-

rier detector with a sensitive area of 9 mm in diameter was used to detect electrons. It was placed at a distance of 69 ± 1 mm from the source. The source had an activity of $8 \mu\text{Ci}$. The Ge(Li) detector was placed at a distance of 112 ± 1 mm from the source. In the second arrangement a silicon surface-barrier detector with a sensitive area of 18 mm diam was used to detect electrons. It was also placed at a distance of 69 ± 1 mm from the source. In this measurement a source of a relatively high initial activity of about $50 \mu\text{Ci}$ was used. The Ge(Li) detector was placed at a distance of 152 ± 1 mm from the source.

The electron detectors were made in our laboratory. The former was a disc of 3500- Ωcm silicon 21 mm diam \times 2.5 mm thick (supplied by Wacker, Burghausen, Germany, bias voltage of 250 V, energy resolution of 6.0 keV for 499-keV K conversion electrons emitted by ^{85}Sr). The latter was a disc of 1200- Ωcm silicon 28 mm diam \times 2.5 mm thick (donated by Soc. des Mines et Fonderies de Zinc de la Vieilles-Montagne, Belgium, bias voltage of 950 V, energy resolution of 5.9 keV). In order to prevent Compton scattering from the electron detector into the photon detector, a lead shield was placed between them.

An Ortec model 403 discriminator was used in the electron branch. It was set at a level corresponding to about 110 keV. In the range of measurements (electrons from 375 to about 500 keV) its jitter in triggering was small. An Ortec model 453 constant fraction timing discriminator was used in the photon branch. Some difficulties encountered in the measurements were due to the very low threshold level used. When the discriminator was set at "delayed" or "prompt" reset, multiple triggering was observed, which caused excessive random coincidences. Therefore, most of the measurements were performed with the discriminator at "external" reset. At this setting

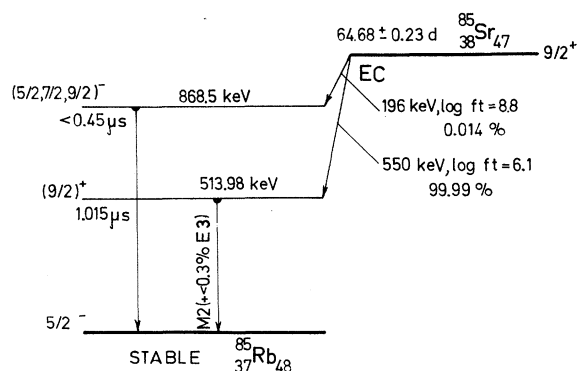


FIG. 1. Decay scheme of ^{85}Sr .

the dead time of the discriminator was about 45 μs . Some dead-time losses were observed in the measurements because of the high triggering rate. In the course of measurements with the second arrangement the threshold level of the photon discriminator was adjusted several times, in order to have a triggering rate of about 8000/sec. Initially, the threshold level corresponded to a photon energy of about 29 keV. As the source decayed, the level was lowered several times and finally reached a value corresponding to about 16 keV. The results of each setting were separately analyzed and corrected for the response of the photon discriminator. Figure 2 shows the response of the photon discriminator as a function of photon energy when the 50% point of the maximum probability of triggering was at 16 keV. Such curves were determined at each setting by measuring the self-gated and direct spectra under experimental conditions.

The time resolution of the system (2τ) obtained in the measurements was about 32 ns. The peaks of the coincidence curves were asymmetrical, with a long tail corresponding to the photon discriminator (mainly due to the coincident detection of low-energy photons).

About 30 and about 1800 coincidences were recorded per hour in the first and second arrangements, respectively. The recording system used a paper tape punch (supplied by Creed and Company, Ltd, England) with an asynchronous speed of 30 characters per second (4 characters were used per record). Therefore, the dead-time losses caused by the recording system amounted to about 7% in the second arrangement.

Checks of the stability of gain of the system were performed daily, while general checks, in particular tests of the three-dimensional analyzer and of the timing discriminator, were performed about twice a month.

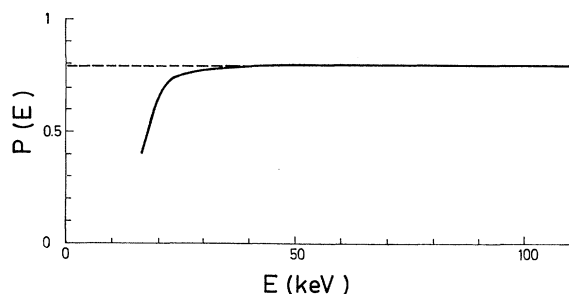


FIG. 2. Response of the photon discriminator as a function of the photon energy, determined from the ratios of counting rates in the same channels of the self-gated and direct photon spectra.

ANALYSIS OF THE DATA

The identification of events due to $e\gamma$ decay was based on the condition of simultaneity and on the energy relation

$$E + E_e = W_0 - B_e. \quad (1)$$

Here E and E_e are the photon and electron energies, respectively, W_0 is the transition energy, and B_e is the binding energy of the electron in the shell from which it was ejected.

The system allowed the resolution of the data due to $e\gamma$ decay involving K -shell electrons ($K\gamma$ decay) from the data involving higher-shell electrons [$(L+M+N)\gamma$ decay]. The three-dimensional tables obtained from the recorded data were analyzed, as described in Ref. 2. On the basis of the analysis described in Ref. 3 and the data of Aiginger,¹¹ the contribution to the counting rates of the external bremsstrahlung of conversion electrons in the source, source backing, and in surrounding materials was estimated to be negligible. The major contribution was expected from the external bremsstrahlung of conversion electrons in the walls of the vacuum chamber, but the estimates indicate that only about 0.043 and 0.075% of counts

in the energy range which we investigated are to be attributed to this effect in the first and second arrangement, respectively.

The differential coefficient of $e\gamma$ decay was determined from the spectra of photons obtained in $e\gamma$ decay by the relation

$$\frac{dB_e}{dE d\Omega}(E, \Theta_0) = N_{e\gamma}(E, \Theta_0) / N_e \Omega(E) \Delta E \epsilon_\gamma P(E) C(E, \Theta_0). \quad (2)$$

Here e stands for K or $L+M+N$, $N_{e\gamma}(E, \Theta_0)$ is the counting rate of $e\gamma$ events in an energy interval at the photon energy E of a width ΔE , N_e is the counting rate of K or $(L+M+N)$ conversion electrons detected in the silicon surface-barrier detector, and $\Omega(E)$ is the effective solid angle of the photon detector (including the geometrical, absorption, and detection-efficiency factors). ϵ_γ is the counting efficiency of the system determined from dead-time losses of the recording system, $P(E)$ is the efficiency of the photon discriminator (see Fig. 2), and $C(E, \Theta_0)$ is the finite-geometry correction factor. It was assumed that the coincidence efficiency was equal to one (the resolving time of the coincidence unit was set at about 200 ns), that the detection efficiency of the electron detectors

TABLE I. $K\gamma$ differential coefficients for the $e\gamma$ decay of the 514-keV state in ^{85}Rb [in units of $10^{-3} \times (mc^2 \text{sr})^{-1}$].

E (keV)	$\frac{dB_{K\gamma}}{dE d\Omega}(E, \Theta_0 = 30^\circ)$
19.5	10.9 ± 6.6
23.6	12.1 ± 5.0
27.7	13.0 ± 4.5
31.6	11.3 ± 4.2
36.1	5.4 ± 1.2
39.5	5.7 ± 1.7
43.5	5.9 ± 1.3
47.5	4.6 ± 1.2
51.5	4.0 ± 1.2
55.5	4.0 ± 1.0
59.5	2.7 ± 0.7
63.5	2.3 ± 0.8
67.5	1.8 ± 0.6
71.5	2.9 ± 0.8
75.5	3.2 ± 0.7
79.5	2.3 ± 0.8
83.6	1.6 ± 0.7
87.5	1.9 ± 0.7
91.6	1.9 ± 0.6
95.5	2.4 ± 0.7
99.6	2.5 ± 0.6
104.5	1.8 ± 0.5
110.4	1.5 ± 0.4
117.4	1.4 ± 0.4
125.5	1.3 ± 0.4
132.5	0.7 ± 0.6

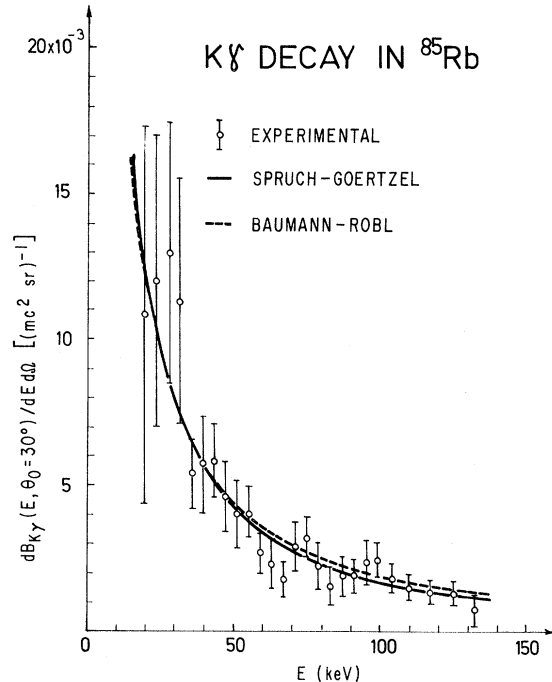


FIG. 3. Differential coefficients of $K\gamma$ decay in ^{85}Rb at a relative angle of emission of 30° . The curves show the values calculated from the theory of Spruch and Goertzel (full curve) and from the theory of Baumann and Robl (dashed curve).

TABLE II. Integrated differential coefficients for $K\gamma$ decay in ^{85}Rb at 30° [in units of $10^{-3} \times \text{sr}^{-1}$].

Range of integration E_1 to E_2 (keV)	$\int_{E_1}^{E_2} \frac{dB}{d\Omega dE} dE$		
	Spruch-Goertzel	Baumann-Robl	This experiment
19.5 to 132.5	0.837	0.866	0.891 ± 0.088
36.1 to 132.5	0.530	0.564	0.515 ± 0.033

did not depend on electron energy in the range from 350 to 500 keV,¹² and that the triggering efficiency of the electron detector did not vary in the same range of energy.

Equation (2) is the same as Eq. (2) in Ref. 2 except for two additional factors [ϵ_γ and $P(E)$], which were introduced because of the relatively high counting rates.

The counting rates of conversion electrons N_e were determined from direct measurements of pulse-height spectra from the electron detector. The detection efficiency of the Ge(Li) detector for photons was determined in the same geometry as in the experiment using a set of calibrated sources of ^{133}Ba , ^{57}Co , ^{137}Cs , and ^{241}Am . ϵ_γ was calculated from the counting rate and the dead time of the recording system of 0.14 s. The finite-geometry factor $C(E, \Theta_0)$ was calculated from the geometry of the system (the source and the detectors), assuming the theoretical ϵ_γ differential coefficients of Spruch and Goertzel.⁴ With this assumption, the correction factor $C(E, \Theta_0)$ is almost independent of photon energy and amounts to 0.95 and 0.96 at the angle Θ_0 of 30° in the first and second arrangement, respectively.

TABLE III. $(L+M+N)\gamma$ differential coefficients for the $\epsilon\gamma$ decay of the 514-keV state in ^{85}Rb [in units of $10^{-3} \times (\text{mc}^2 \text{sr})^{-1}$].

E (keV)	$\frac{dB_{(L+M+N)\gamma}}{dE d\Omega}(E, \Theta_0 = 30^\circ)$
27.5	17.4 ± 7.8
33.5	4.4 ± 5.7
39.5	5.7 ± 2.6
47.8	3.1 ± 2.1
55.8	3.5 ± 2.3
63.8	3.4 ± 2.1
73.8	3.2 ± 1.5
85.8	3.3 ± 1.3
97.8	2.5 ± 1.2
109.8	2.6 ± 1.5
121.8	2.4 ± 1.4
131.7	1.2 ± 2.9

RESULTS AND DISCUSSION

The channel width in both branches was approximately 2.0 keV. In order to improve statistics, averages were taken over two channels up to 100 keV, and over three channels for higher energies. Table I and Fig. 3 show the results for $K\gamma$ decay from all measurements. Figure 3 also shows the values derived from the theory of Spruch and Goertzel⁴ (full curve) and those from the theory of Baumann and Robl⁵ (dashed curve).

The values of the experimental and theoretical differential coefficients were integrated over two energy intervals, and the results are given in Table II.

The experimental results in the range of energies we investigated are in agreement with the theory of Spruch and Goertzel and the theory of Baumann and Robl. This indicates that the dominant contribution to $K\gamma$ decay in the $M2$ transition in ^{85}Rb comes from electronic intermediate states, i.e., this $K\gamma$ decay proceeds mainly as the internal Compton effect.

In the first arrangement the statistics of data from $(L+M+N)\gamma$ decay was insufficient. There-

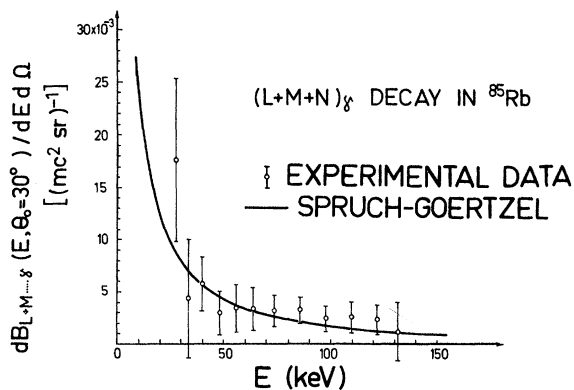


FIG. 4. Differential coefficients of $(L+M+N)\gamma$ in ^{85}Rb at a relative angle of emission of 30° . The full line was calculated from the theory of Spruch and Goertzel for $K\gamma$ decay.

fore, only the data from the second arrangement were analyzed. Table III and Fig. 4 show the results averaged over three, four, and five channels. Figure 4 also shows the theoretical values derived from the estimate of Spruch and Goertzel. According to this estimate the differential coefficients of decay for higher-shell electrons are approximately equal to the differential coefficients for $K\gamma$ decay.

The value of the differential coefficients for $(L+M+N)\gamma$ decay, integrated over an energy interval of 27.5 to 131.7 keV calculated from the experimental data, is equal to $(0.84 \pm 0.16) \times 10^{-3} \text{ sr}^{-1}$. This is in reasonable agreement with the corres-

ponding value of $0.67 \times 10^{-3} \text{ sr}^{-1}$ calculated from the theory of Spruch and Goertzel for $K\gamma$ decay.

ACKNOWLEDGMENTS

The authors thank the Electronics Department of the "Rudjer Bošković" Institute for the maintenance of the three-dimensional analyzer, the firm Soc. des Mines et Fonderies de Zinc de la Vieilles-Montagne for the donated discs of large-diameter silicon for surface-barrier detectors, Mrs. N. Ilakovac for the preparation of the detectors, and I. Čelig for his help with the equipment in the Laboratory.

*Research supported by the Council for Scientific Research of S. R. Croatia, Zagreb, Yugoslavia.

- ¹T. Lindqvist, B. G. Pettersson, and K. Siegbahn, *Nucl. Phys.* **5**, 47 (1958); E. Fuschini, C. Maroni, and P. Veronesi, *Nuovo Cimento* **26**, 831 (1962); **41B**, 252 (1966); A. Ljubičić, B. Hrastnik, K. Ilakovac, V. Knapp, and B. Vojnović, *Phys. Rev.* **187**, 1512 (1969); A. Ljubičić, B. Hrastnik, K. Ilakovac, M. Jurčević, and I. Basar, *Phys. Rev. C* **3**, 824 (1971).
- ²M. Jurčević, K. Ilakovac, and Z. Krečak, *Phys. Rev. C* **9**, 1611 (1974).
- ³M. Jurčević, K. Ilakovac, and Z. Krečak, *Phys. Rev. C* **11**, 1312 (1975).
- ⁴L. Spruch and G. Goertzel, *Phys. Rev.* **94**, 1671 (1954).

- ⁵V. K. Baumann and H. Robl, *Z. Naturforsch.* **9a**, 511 (1954).
- ⁶D. P. Grechukhin, *Yad. Fiz.* **4**, 42 (1966) [*Sov. J. Nucl. Phys.* **4**, 30 (1967)], and references quoted therein.
- ⁷J. D. Horen, *Nucl. Data* **B5**, 131 (1971).
- ⁸G. H. Miller, P. Dillard, M. Eckhouse, and R. E. Welsh, *Nucl. Instrum. Methods* **104**, 11 (1972).
- ⁹E. Vatai, A. C. Xenoulis, K. R. Baker, F. Tolea, and R. W. Fink, *Nucl. Phys.* **A219**, 595 (1974).
- ¹⁰T. Alvåger, H. Ryde, and P. Thieberger, *Ark. Fys.* **21**, 559 (1962).
- ¹¹H. Aiginger, *Z. Phys.* **197**, 8 (1966).
- ¹²B. Planskoy, *Nucl. Instrum. Methods* **61**, 285 (1968); J. B. Willet, *ibid.* **84**, 157 (1970).